Shifting Input Filter Resonances - An Intelligent Converter Behavior for Maintaining System Stability

Mario Schweizer and Johann W. Kolar
Power Electronic Systems Laboratory
Swiss Federal Institute of Technology (ETH Zurich),
Physikstrasse 3,
8092 Zurich, Switzerland
Email: schweizer@lem.ee.ethz.ch

***Abstract*—Instead of just transforming energy, a modern power converter should incorporate enhanced features to adapt its behavior to its environment. Stability issues in 3-phase power systems with PFC rectifiers incorporating input filters have been a problem for a long time. In this paper a new concept is presented as to how the power converter can shift filter resonances into an unproblematic frequency range by simulating an additional inductivity or capacity. The concept is proved with an extensive stability analysis in the synchronous dq-reference frame. Simulations in the time domain demonstrate the positive impact of the proposed method.**

***Index Terms*—Stability, resonance shifting, active damping, three-phase AC**

I. Introduction

Stability issues in interconnected DC-DC power conversion systems have been a research topic for a long time. Amongst others, problems such as stable converter control with an input EMI filter, stable converter operation when connected to a weak power source with high output impedance and stable converter operation of multiple DC-DC converters connected to a common DC power distribution bus [1] have been analyzed in depth. Most of these issues and their mathematical descriptions are well known and understood. Simple to use design theorems such as Middlebrook's impedance criterion [2] have been derived from linear time-invariant system theory to guarantee system stability. They are based on the comparison of input and output impedances at an arbitrary system interface. In most cases the small signal analysis is sufficient to determine stability as the DC-DC converters work at a constant working point [3].

Amongst the simple theories, the direct physical interpretation of the input impedance has also led to a good acceptance. The input impedance can be determined with measurement methods directly on the system boundaries. On the basis of the impedance comparison, filter design rules have been derived. These allow for the design of EMI filters which comply with specific norms and have a neligible impact on the control. Because the converter is behaving like a constant power load, which can be described simply by a negative resistance in the small signal analysis, the interconnection of an EMI filter and the power converter is prone to unstable behavior.

A stable filter design often requires damping resistors which lead to additional losses and volume. Various active damping methods have been proposed and implemented [4]. These are able to change the converter behavior in such a way that the filter resonance is damped and the physical damping resistor can be omitted.

More recent research topics cover the stability analysis of single phase AC-DC converters with PFC [5]. The discussion of these systems is more involved because of their time varying nature which makes the linearization around a constant working point impossible. Several approaches have been proposed so far. The problem has roughly been divided into two frequency regions.

For distortions in a frequency range below the fundamental mains frequency, a reduced order model has been proposed [6]. The main idea is to consider the envelope of the AC input signals, covering a low frequency small signal deviation of the signal amplitudes from the steady state value. The current control is considered to work ideally for the derivation of this model. The impedance ratio criterion was applied to guarantee system stability with this reduced order model.

However, in a recent publication it was shown that it is not correct to apply the impedance criterion on this reduced order model [7]. The amplitude modulation corresponds to the simultaneous injection of two small signal waveforms with frequency components of $(\omega_s+\omega_e)$ and $(\omega_s-\omega_e)$ which results in a nonconform impedance definition. The authors propose a different large signal model to solve this problem.

When distortions occur in a frequency range above the fundamental frequency several reduced order models have been proposed [8], [9]. The DC-link voltage is often assumed to be constant and only the current control loop is considered for the derivation. The main problem in this frequency range is finding an appropriate operating point for the system linearization. One way is to use a set of points on the AC input voltage waveform for linearization and guarantee for small signal stability for all points. This is especially difficult at the zero crossing of the input voltage. Another approach is to use an averaged operating

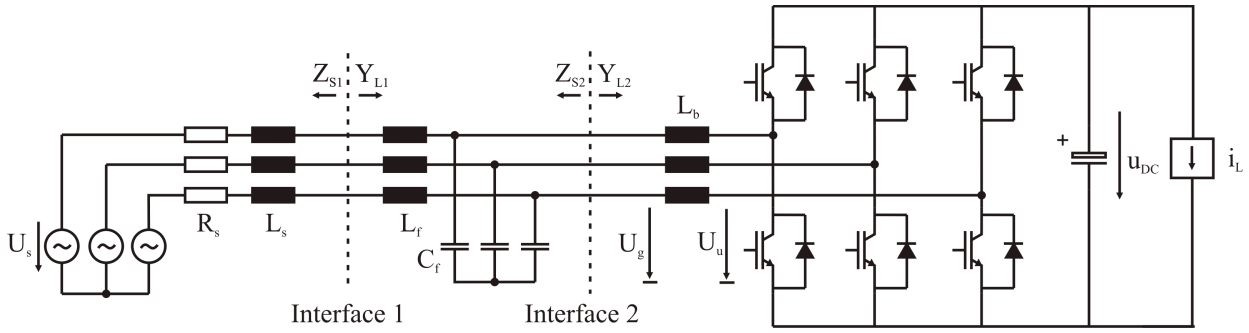

Fig. 1. Sample system consisting of weak source, EMI filter and PFC rectifier

point for linearization. This averaged operating point corresponds to the rms input voltage. It is questionable if it is sufficient to show the small signal stability for this averaged operating point in order to guarantee the stability of the entire system.

Several active damping schemes have been proposed and implemented for single phase AC-DC converters. A comprehensive overview on stability issues and active damping in DC and single phase AC systems is given in [10].

The least understood systems in terms of stability assessment are clearly 3-phase AC-DC PFC converters. In 3-phase systems all phases are coupled if the star point is not connected to the neutral, which is most often the case. This prevents the treatment of the 3-phase rectifier as a single phase system. Nevertheless, this is the way it is most often done in practice. However, the coupling of the three phases is neglected and the problem of finding an appropriate linearization operating point still persists with this method. This is also an unsolved issue of the proposed method in [11]. There a description of the 3-phase PFC rectifier with two parallel DC-DC converters was proposed.

An interesting approach for determining the stability of 3-phase AC-DC converters was shown in [12]. If the transformation in the synchronous dq-reference frame is applied, the varying AC variables voltage and current are transformed into a constant operating point. This allows for a correct linearization of the system around this operating point, resulting in a linear MIMO system description. System stability can be assessed by observing the eigenvalue plots over frequency of the transfer matrix, known as the generalized Nyquist criterion. It is also possible to use complex transfer functions [13] in dq-coordinates for fully symmetric systems. This approach is equivalent to the matrix description except that non-symmetric systems, i.e. active rectifier with outer voltage control loop, cannot be described [14].

Belkhayat [12] developed a similar method to the DC impedance criterion for the 3-phase AC system described in the dq-reference frame. If a matrix norm is applied to the output impedance and input admittance matrices at an arbitrary system interface, a criterion for system stability can be deduced equivalent to Middlebrook's theorem. In [15], this criterion was applied to assess the system stability of a 3-phase active rectifier with an input filter. Lately, the approach has been generalized to single phase AC-DC converters with the introduction of an artificial rectangular axis [16].

The high complexity and the difficult physical interpretation of the impedance matrices prevented this method from wider usage. However, in a recent publication a simple method for accurate measurement of the impedance matrix elements was proposed and implemented [17], and refined in [18].

Some methods for active damping have been proposed [19] for the 3-phase AC-DC PFC rectifier. Among approaches with simple compensation measures having nonlinear precontrol terms [20], an interesting concept is the virtual resistor [21], [22]. In order to guarantee a stable current control with an input filter, the resonances of the filter have to be damped. This usually leads to additional components, filter volume and increased losses. The rectifier simulates a resistor at its input terminals with the virtual resistor approach, damping the resonance actively. A similar approach with a so called negative inductor has been mentioned in [23] for a current source converter.

In this paper the virtual resistor concept is extended to a general virtual impedance concept, a more intelligent converter behavior. As a modern 3-phase power converter can simulate nearly an arbitrary input impedance, it makes sense to define a converter behavior which takes advantage of this. By use of a simulated capacitor or inductor it is possible to move filter resonances out of the critical region, where an unstable system interaction could occur. This is a new insight as it allows for a different converter behavior depending on the frequency range. It divides the standard PFC rectifier behavior, meaning the input current has to be always in phase to the input voltage, to a frequency dependant one.

The virtual impedance concept will be explained using impedance matrices. Therefore a short recapitulation of the stability theory and the impedance criterion in the dq reference frame will be presented in section II. In order to apply the impedance criterion the output impedance of the EMI filter and the input admittance of the active rectifier are derived in section III and IV. The impact of several effects like time delays and current and voltage regulation bandwidth are highlighted. In section V the virtual impedance concept is explained. The benefits of an intelligent converter behavior concerning damping and resonance shifting is shown. Finally, in section VI the concept is proven with a time domain simulation.

TABLE I
MAIN PROPERTIES OF SAMPLE RECTIFIER SYSTEM.

Component	Value
R_s	$50\,\mathrm{m\Omega}$
L_s	$50\,\mu\mathrm{H}$
L_f	$500\,\mu\mathrm{H}$
C_f	$40\,\mu\mathrm{F}$
L_b	$600\,\mu\mathrm{H}$
C_{dc}	$1\,\mathrm{mF}$
f_s	$50\,\mathrm{kHz}$
U_N	$230\,\mathrm{V_{rms}}$
U_{DC}	$700\,\mathrm{V}$

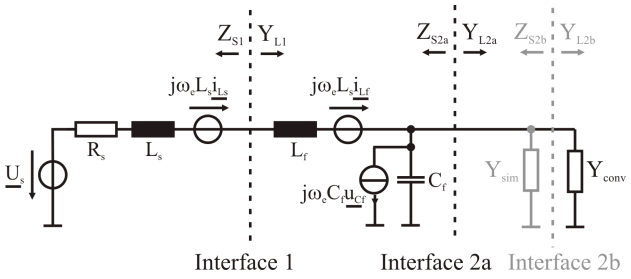

Fig. 2. Equivalent circuit in synchronous dq-reference frame.

II. STABILITY IN 3-PHASE SYSTEMS

The new concept will be demonstrated with a sample system consisting of a source with internal impedance, a LCL filter topology and the 3-phase active rectifier depicted in Fig. 1. The main properties of the filter and the converter are summarized in table I. Modern power semiconductors allow for an increased switching frequency maintaining a high efficiency and make it possible to have a very fast current control bandwidth. Although the EMI filter components are over-dimensioned for the assumed switching frequency of 50 kHz, this situation can occur if a cheap standard filter stage is ordered from an external manufacturer.

In order to assess the stability of this system the full dynamics including control and passive components could be considered observing all closed loop poles of the system. The drawback of this method is that the separation into subsystems and the localisation of possible problematic interactions is quite difficult. The frequency information is lost and the complete analytical description of the system has to be known. Hardware measurements can not be used to assess the system stability.

It would be desirable to have a similar method to Middlebrooks impedance criterion for input filter design in DC systems. There the modulus of the input and the output impedance at a specific system interface are compared and statements concerning the stability can be made. The source of possible problematic interactions can be identified and countermeasures can be implemented. It is possible to measure the impedances at the system interface and gather information on the subsystems without knowing the complete internal behavior.

Middlebrooks impedance criterion is derived from the Nyquist plot in which the ratio Z_{out}/Z_{in} is plotted in the imaginary plane and the anti clockwise encirclements of the point -1 is counted. If this number is equal to the openloop poles of Z_{out}/Z_{in} than the system is stable. If the modulus of the ratio Z_{out}/Z_{in} is limited to one, the critical point is never encircled. It is obvious that this leads to a quite restrictive criterion. Further enhancements of the impedance criterion exist where the allowed area is enlarged and also the phase margin is considered in order to have a less restrictive criterion for stability [24].

If the synchronous reference frame transformation is applied to a 3-phase system all variables transform to a stationary operating point. The system can now be described as a linear, time invariant MIMO system with just 2 state variables and all the rules for stability of MIMO systems apply. Impedances transform to 2x2 matrices. If we select a specific interface and consider the output impedance matrix and the input admittance matrix than the voltage at the interface is given by

$$u_g = [I + Z_{out} \cdot Y_{in}]^{-1} \cdot H_{qd} \cdot u_s \tag{1}$$

The generalized Nyquist criterion states for MIMO system that the system is closed loop stable if the anti-clockwise encirclement of -1 by the set of eigenvalues of the return ratio $Z_{out} \cdot Y_{in}$ is equal to the total number of right half plane poles of $Z_{out} \cdot Y_{in}$.

The number of open loop unstable poles is zero for most practical systems. As for the SISO case, we can now define a matrix norm which includes the maximum eigenvalues and limit it to be lower than one, so that no eigenvalue plot can encircle the critical point -1. The following condition holds for the eigenvalues of a matrix G, whereas $\overline{\sigma}$ and $\underline{\sigma}$ denote the maximum respective minimum singular value of the matrix.

$$\underline{\sigma}(G) \leq |\lambda_i(G)| \leq \overline{\sigma}(G) \tag{2}$$

An appropriate impedance criterion for stability at the corresponding interface can be found with this condition.

$$\overline{\sigma}(Z_{out}) \cdot \overline{\sigma}(Y_{in}) < 1 \tag{3}$$

$$\overline{\sigma}(Z_{out}) < \frac{1}{\overline{\sigma}(Y_{in})} \tag{4}$$

By use of the identity for singular values of the matrix inverse $1/\overline{\sigma}(G) = \underline{\sigma}(G^{-1})$ the impedance criterion can also be expressed as:

$$\overline{\sigma}(Z_{out}) < \underline{\sigma}(Z_{in}) \tag{5}$$

The maximum singular value norm is equal to the maximum gain of the matrix into d- or q-direction meaning the dominant element of the matrix. It is obvious that this impedance criterion has the same conservative nature as Middlebrook's impedance criterion because the major part of the imaginary plane is actually forbidden. A simple phase margin definition would be useful to enlarge the allowed region and find a less restrictive condition.

III. EMI FILTER OUTPUT IMPEDANCE

In order to apply the impedance criterion we have to compute or measure the source and load impedances at a specified interface. It is quite simple to calculate them if we first introduce the matrices for the simplest possible elements, in particular a resistor, an inductor and a capacitor.

$$Z_R = \begin{pmatrix} R & 0 \\ 0 & R \end{pmatrix} \tag{6}$$

$$Z_L = \begin{pmatrix} sL & -\omega_e L \\ \omega_e L & sL \end{pmatrix} \tag{7}$$

$$Y_C = \begin{pmatrix} sC & -\omega_e C \\ \omega_e C & sC \end{pmatrix} \tag{8}$$

As with normal impedances, rules for series and parallel connection of impedance or admittance matrices apply. For series connection of elements, the impedance matrices add together and for parallel connection of circuit elements the admittance matrices add together:

$$Series: \qquad Z_{sum} = Z_1 + Z_2 \tag{9}$$

$$Parallel: \qquad Y_{sum} = Y_1 + Y_2 \tag{10}$$

The impedance matrix is the inverse of the corresponding admittance matrix and vice versa:

$$Z = Y^{-1} \qquad Y = Z^{-1} \tag{11}$$

Now, the interface impedance matrices can easily be computed. If we consider the equivalent circuit depicted in Fig. 2 we can choose two interfaces for the stability analysis. At interface 1 where the converter is connected with the weak source, instability in the grid voltage can occur. The second interface is between the EMI filter and the power converter where mainly a stable current control is of interest. At interface one the source output impedance can be found:

$$Z_{S1} = Z_{Rs} + Z_{Ls} = \begin{pmatrix} R_S + sL_S & -\omega_e L_S \\ \omega_e L_S & R_S + sL_S \end{pmatrix} \tag{12}$$

At interface 2a the source output impedance is now given by the EMI filter:

$$Z_{S2a} = \left[[Z_{Rs} + Z_{Ls} + Z_{Lf}]^{-1} + Y_{Cf} \right]^{-1} \tag{13}$$

Plotted in Fig. 3 is the singular value norm of the filter output impedance at interface 2, $\overline{\sigma}(Z_{S2})$. It can be noticed that in the synchronous reference frame the single phase filter resonance gets split into two separated resonance peaks. They are aligned at the frequencies $\omega_0 + \omega_e$ and $\omega_0 - \omega_e$ (ω_0: resonance frequency of single phase filter equivalent, ω_e: angular speed of dq-reference frame).

This might not be a problem in a 50 Hz system. In a supply grid with e.g. 800 Hz fundamental, which is possible in aircraft onboard power grid, this resonance split can cause a filter design to fail and should not be neglected. Generally, if the filter resonance frequency and the synchronous reference frame frequency are not separated by a decade or more, it should not be neglected.

IV. VSC Input Admittance

A. Derivation of Y_{L2}

The input admittance matrix of the VSC can be derived with some algebraic effort. The VSC is regulated as an active rectifier with a simple cascaded control structure depicted in Fig. 4. An outer control loop regulates the output DC voltage and two inner control loops regulate

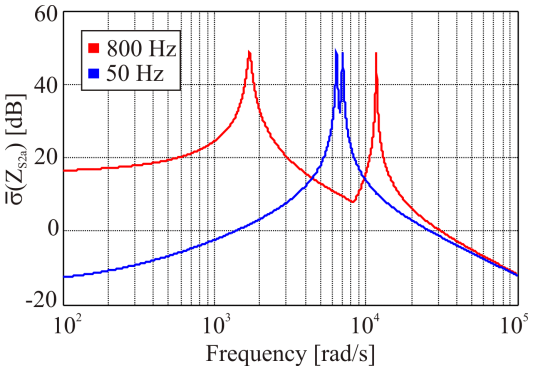

Fig. 3. Filter output impedance Z_{S2}.

the input current d- and q-axis components. The controller equations are as follows:

$$R_i = k_{pi}\frac{1+sT_{ni}}{sT_{ni}}, \; R_u = k_{pu}\frac{1+sT_{nu}}{sT_{nu}} \tag{14}$$

The boost inductor cross-coupling equations and the grid voltage are considered with feedforward of the appropriate values. The PLL for tracking the input voltage reference angle is assumed to have a very low bandwidth and its dynamics are neglected. The steady state angular frequency of the synchronous reference frame is fixed. In steady state, the PLL reference frame d-axis is aligned to the synchronous reference frame and all variations are considered to be small signal deviations.

As the converter model is based on the state space averaging over a switching period, the model is valid for a frequency range below the switching frequency only. The current and voltage sensors are assumed to have a high bandwidth above the converter switching frequency and therefore their transfer functions can be assumed to be unity.

$$H_i = 1, \; H_u = 1 \tag{15}$$

In a real setup the control is computed on a DSP with a fixed sampling rate. It is therefore inevitable to have a certain time delay in the control loop. The modulation of the converter output voltage introduces an additional time delay. Unfortunately, the space vector modulation (SVM) and PWM lead to a coupling between the d- and q-axis and the introduced time delay can be time-varying also in the synchronous dq-reference frame [25]. We neglect this cross-coupling (it is small anyway) and consider as the worst case the largest time delay consisting of computation time and SVM equally in d- and q-axis with the transfer function G_t.

$$G_t = e^{-sT_t} \approx \frac{1}{1+sT_t} \tag{16}$$

No further assumptions are made for the derivation of the VSC equations. In particular, there is no assumption about the converters q-axis current or voltage being zero.

The input admittance matrix is given by:

$$\begin{pmatrix} i_d \\ i_q \end{pmatrix} = \begin{pmatrix} Y_{dd} & Y_{dq} \\ Y_{qd} & Y_{qq} \end{pmatrix} \cdot \begin{pmatrix} u_{gd} \\ u_{gq} \end{pmatrix} \tag{17}$$

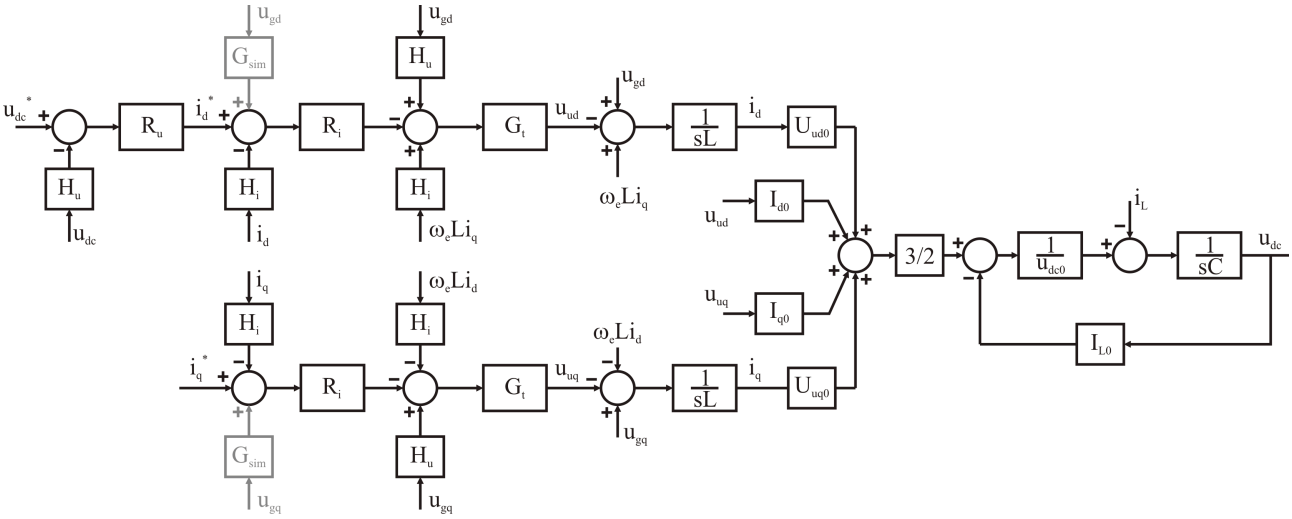

Fig. 4. Block diagram of rectifier and control.

The linearized system equations can be found with Fig. 4.

$$i_d = \frac{1}{sL}\left(u_{gd} + \omega_e L i_q - u_{ud}\right) \tag{18}$$

$$i_q = \frac{1}{sL}\left(u_{gq} - \omega_e L i_d - u_{uq}\right) \tag{19}$$

$$u_{ud} = G_t\left(u_{gd} + \omega_e L i_q - \left(i_d^* - i_d\right) R_i\right) \tag{20}$$

$$u_{uq} = G_t\left(u_{gq} - \omega_e L i_d - \left(-i_q\right) R_i\right) \tag{21}$$

$$i_d^* = -u_{dc} R_u \tag{22}$$

$$u_{dc} = G_p\left(I_{d0} u_{ud} + U_{ud0} i_d + I_{q0} u_{uq} + U_{uq0} i_q\right) \tag{23}$$

$$G_p = \frac{3}{2}\frac{1}{U_0 sC + I_0} \tag{24}$$

Note that the active power is built with the converter voltage u_u and not with the voltage applied before the boost inductor u_g. In order to determine Y_{dd} and Y_{qd} we set u_{gq} to zero and solve for the corresponding equations.

$$i_q = \underbrace{\frac{G_t - 1}{G_t R_i + sL}\omega_e L}_{a_1} i_d \tag{25}$$

$$u_{uq} = \underbrace{\frac{-G_t\left(R_i + sL\right)}{G_t R_i + sL}\omega_e L}_{a_2} i_d \tag{26}$$

$$u_{ud} = \underbrace{\frac{-G_t\left(sL + R_i\left(1 + R_u G_p\left(U_{ud0} + a_1 U_{uq0} + a_2 I_{q0}\right)\right)\right)}{\left(G_t - 1\right) + G_t R_i R_u G_p I_{d0}}}_{a_3} i_d \tag{27}$$

The first two admittance matrix elements can be expressed in a simple form. Parameter a_1 describes the impact of the dead time resulting in an incomplete compensation of the cross coupling and parameter a_3 is related to the complete active power feedback through the outer DC-voltage loop.

$$Y_{dd} = \frac{1}{a_3 - a_1\omega_e L + sL} \tag{28}$$

$$Y_{qd} = \frac{a_1}{a_3 - a_1\omega_e L + sL} \tag{29}$$

In order to determine Y_{qq} and Y_{dq} we set u_{gd} to zero and solve for the corresponding equations. We introduce some parameters:

$$i_d = \underbrace{\frac{-G_t R_i R_u G_p\left(b_3 I_{q0} + U_{uq0} + \omega_e L I_{d0}\right) + \left(1 - G_t\right)\omega_e L}{G_t R_i + sL + G_t R_i R_u G_p\left(U_{ud0} - sL I_{d0}\right)}}_{b_1} i_q \tag{30}$$

$$u_{ud} = \underbrace{\frac{-G_t\left(R_i R_u G_p\left(b_1 U_{ud0} + U_{uq0} + b_3 I_{q0}\right) + b_1 R i + \omega_e L\right)}{G_t R_i R_u G_p I_{d0} - 1}}_{b_2} i_q \tag{31}$$

$$u_{uq} = \underbrace{\frac{-G_t\left(R_i + sL\right)}{G_t - 1}}_{b_3} i_q \tag{32}$$

The last two admittance matrix elements can also be written in a simple form. Parameter b_1 describes the impact of the time delays and the coupling over the active power feedback loop and b_3 is related to the current loop in q-direction.

$$Y_{qq} = \frac{1}{b_3 + b_1\omega_e L + sL} \tag{33}$$

$$Y_{dq} = \frac{b_1}{b_3 + b_1\omega_e L + sL} \tag{34}$$

If we would assume no time delay ($G_t = 1$) several simplifications would be possible: among others $Y_{qd} = 0$ and $Y_{qq} = 0$ due to the ideal decoupling and feedforward control. Y_{dq} would not equal zero because of the small coupling via the active power loop.

B. Properties of Y_{L2}

If we have a look at the components of Y_{in} in Fig. 5a one can notice the dominant behavior of Y_{dd} and Y_{qq}. The negative differential resistance behavior of Y_{dd} can be observed for lower frequencies where the converter behaves as a constant power load (voltage control bandwidth $\omega_{b,u} = 500\,\mathrm{Hz}$, current control bandwidth $\omega_{b,i} = 5\,\mathrm{kHz}$). If we disable the feedforward of the grid voltage the impedance changes considerably in the mid-frequency

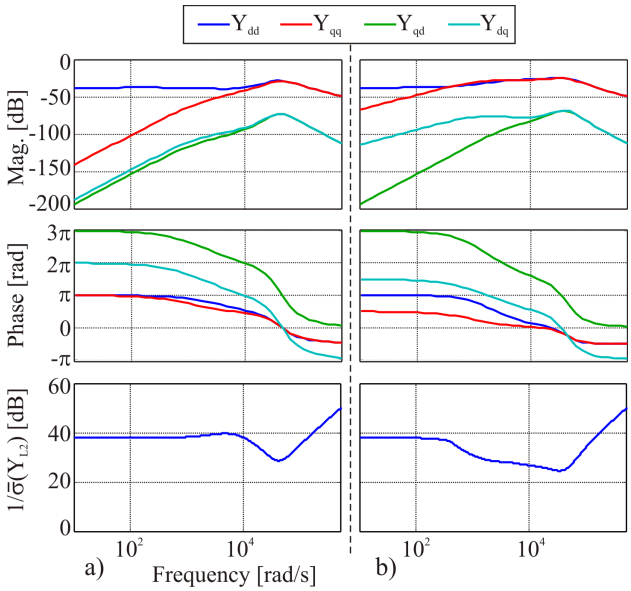

Fig. 5. Converter input admittance matrix components and its corresponding singular value norm. a) With feedforward of grid voltage, b) Without feedforward of grid voltage.

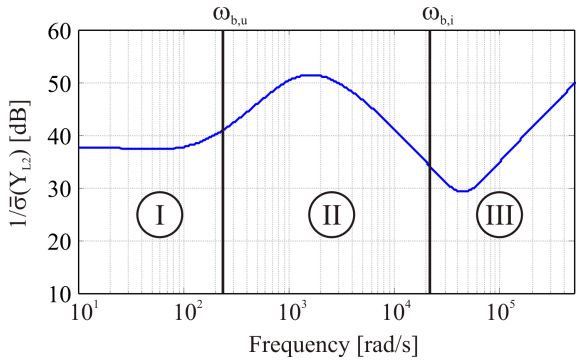

Fig. 6. Frequency ranges of the converter input impedance $\underline{\sigma}(Z_{L2})$.

range (cf. Fig. 5b). The Y_{qq} component now is larger than Y_{dd} for a certain frequency range.

Altough it makes sense to look at the components of the input admittance matrix it is more interesting to look at the matrix norm keeping the impedance criterion in mind.

Considering Fig. 5, the similiarity between the plot of $1/\overline{\sigma}(Y_{L2}) = \underline{\sigma}(Z_{L2})$ and the input impedance of a DC-DC boost converter is obvious since the active rectifier actually is a 3-phase boost regulator.

One can also observe the typical impedance sag caused by the time delay. If the feedforward control of the grid voltage is disabled the admittance norm completely changes. Now a certain part of the admittance matrix is dominated by the Y_{qq} component which also influences the condition for stability.

In Fig. 6 the norm is plotted again in more detail with feedforward control of the grid voltage and a lower DC-link voltage regulation bandwidth of 35 Hz. We can now determine specific frequency ranges where the converter behaves differently.

In section I, below the voltage regulation bandwidth, the constant power load behavior with negative input impedance is dominating. The norm only depends on the consumed power.

The impedance norm decreases with increasing power, possibly rendering the system unstable for a high source impedance in this frequency range. A favorable choice for a stable control is to select the voltage regulation bandwidth as low as possible to limit this critical constant power frequency range and the current regulation bandwidth as high as possible.

In section II, between the voltage regulation bandwidth and the current regulation bandwidth, the converter has a very high input impedance. This is due to the grid voltage feedforward and the current control, which force the input current not to react to changes of the input voltage. In this frequency range the basic behavior of the converter could be freely redefined without affecting the power transfer at the fundamental frequency.

In section III, a frequency range above the current regulation bandwidth, first the time delay effect is obvious and then the boost inductance is dominating. It is difficult to change the input impedance for this frequency range because of the time delays and SVM bandwidth limit.

V. Virtual Impedance Concept

The stability at interface 2a can be assessed if the impedance criterion is applied. In Fig. 8 the filter output impedance matrix norm (blue curve) and the converter input impedance norm (black curve) are depicted. It can be noticed that the filter resonance is only slightly damped by the source series resistor and the impedance criterion is not fulfilled. Stability is not guaranteed.

The before mentioned frequency dependant behavior now allows for changing the converter behavior to an advantageous one. It is basically possible to simulate an arbitrary impedance at the converter terminals for a frequency range below the current regulation bandwidth. The constant power load behavior only has to be maintained for a low frequency range and is directly related to the voltage regulation bandwidth.

In order to simulate an additional circuit element with the converter the control loop has to be changed according to Fig. 4. The input voltage u_g is processed with an additional transfer function G_{sim} and added directly to the current controller reference input. No cross-coupling is introduced as the desirable impact of the simulated circuit element persists although it is neglected.

Again, it is possible to derive the input admittance matrix of the converter $Y_{L2,new}$. The impact of the simulated circuit element can be distinguished from the standard behavior if the new input admittance is split into two parts, the input impedance of the conventionally controlled rectifier Y_{conv} and the additional element Y_{sim} because the two admittance matrices can be thought to be in parallel:

$$Y_{sim} = Y_{L2,new} - Y_{conv} \tag{35}$$

The resulting expression contains the simulated transfer function G_{sim} in d- and q-axis direction disturbed by the active power feedback loop. Due to space limitations the equation is not given here. In the previously favored frequency range II, $Y_{sim,dd}$ and $Y_{sim,qq}$ are nearly equal

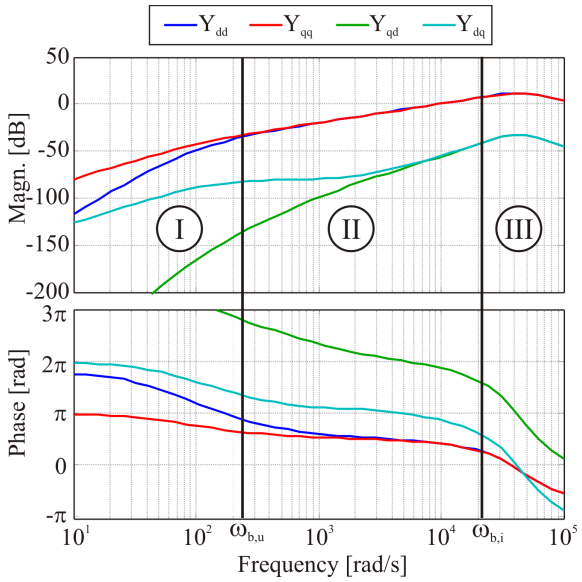

Fig. 7. Simulated admittance matrix elements Y_{sim} for $C = 100\,\mu$F.

to the desired transfer function G_{sim}. As an example Fig. 7 shows the admittance matrix components of a simulated capacitor ($C_{sim} = 100\,\mu$F).

In order not to disturb the converter behavior in the low frequency and very high frequency range, a bandpass filter is useful. Especially for a discrete implementation in simulation or on a DSP the damping of high frequency noise is necessary if a virtual capacitor is simulated since it includes the computation of a discrete derivative which is very sensitive to high frequency noise.

$$G_{sim,f} = \frac{sT_l}{1+sT_l}\frac{1}{1+sT_h}G_{sim} \tag{36}$$

Interface 2a can now be moved to the new location 2b (cf. Fig. 2) for the stability analysis. The simulated admittance can be viewed as a part of the EMI filter network. This can be calculated by adding Y_{sim} to the filter output impedance matrix as follows:

$$Z_{S2,new} = \left[[Z_{Rs} + Z_{Ls} + Z_{Lf}]^{-1} + Y_{Cf} + Y_{sim}\right]^{-1} \tag{37}$$

It is now possible to exploit all possible benefits of having an arbitrary artificial circuit element in parallel to the filter capacitor. The obvious choice of the simulated element is a damping resistor, resulting in the virtual resistor damping method. Other choices could be an additional capacitor, an additional inductor, both possibly damped or even a combination of several elements. In Fig. 8 the influence of a simulated virtual resistor, a capacitor and an inductor on the filter output impedance is shown.

The virtual resistor allows for damping the filter resonance. Its positive impact can be visualized very nicely with Fig. 8. If we compare the converter input impedance (black curve) with the virtually damped filter output impedance (green) the increased gain margin can be seen. In contrast to the initial filter output impedance (blue) the stability condition is now fulfilled.

A different application of the virtual impedance concept is possible if we operate from a distorted line. Imagine

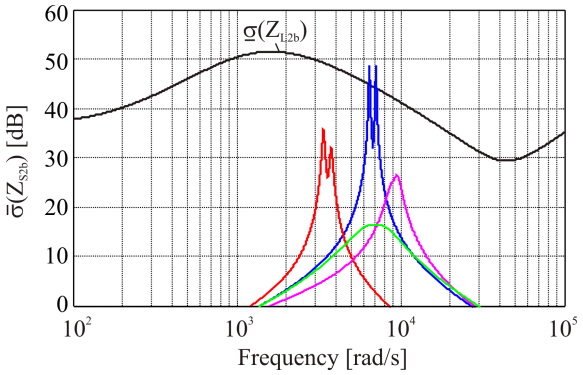

Fig. 8. Filter output impedance with simulated virtual circuit elements (green: $10\,\Omega$, red: $100\,\mu$F, magenta: $600\,\mu$H).

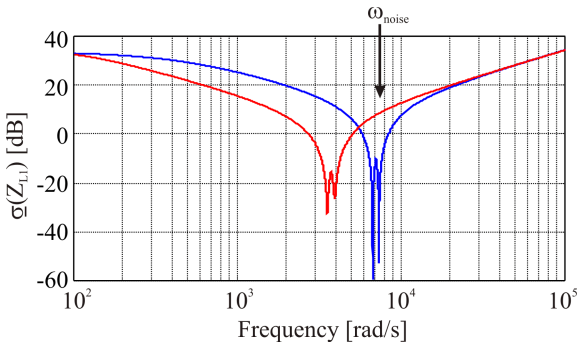

Fig. 9. Input impedance at interface 1. Shifted resonance with simulated capacitance $C_{sim} = 100\,\mu$F (red curve).

a plant where your converter is connected to a supply grid with other converters already operating. If one of these converters injects harmonics, possibly near the filter resonance frequency, it could be useful to move the resonance frequency in order to limit the harmonic currents and get a sinusoidal converter input voltage. This can be achieved without physically changing the input filter: just a simulated additional capacitor, to move the resonance frequency to a lower value, is necessary.

It is also possible to shift the resonance frequency to a higher value if a virtual inductor is simulated. In this case it is beneficial to simulate a resistor in series to the inductor in order not to generate an undamped LC resonance. In Fig. 9 the resonance shift to a lower frequency with a simulated capacitor is shown.

The effect is similar to the virtual resistor damping concept except that no additional power is absorbed at the harmonic frequency. The input impedance at interface 1 is increased so that harmonics will be bypassed to the power source.

VI. Time Domain Simulation

In order to prove the resonance shifting concept, a time domain simulation with Simulinks SimPowerSystems library is built. The necessary high current control bandwidth can be achieved with a switching frequency of 50 kHz. A 3-phase voltage noise source with 1 V amplitude and a frequency of 1175 Hz (near the original filter resonance frequency) was capacitively coupled to the circuit at interface 1 to simulate the distorted line condition.

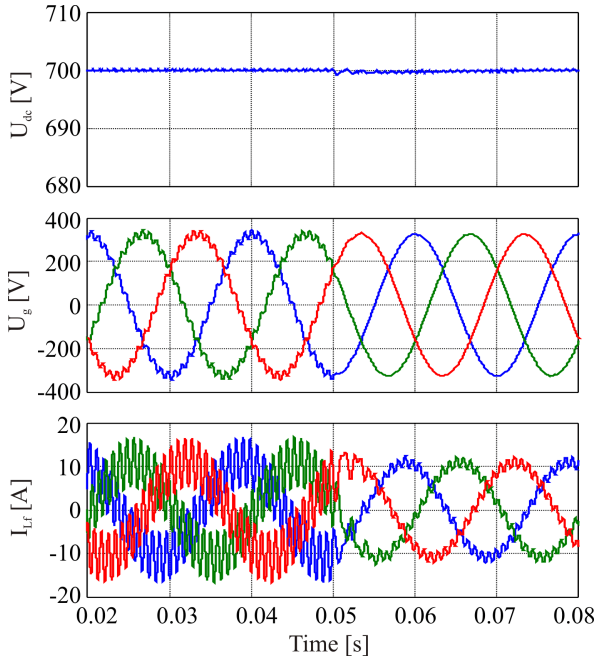

Fig. 10. Time domain simulation of damping concept with resonance shifting ($C_{sim} = 100\,\mu$F).

As a result, the current and the input voltage over the filter capacitor are highly distorted (cf. Fig. 10). At the time instant t=0.05s the virtual capacitor is activated and the distortions are significantly reduced. The filter capacitor voltage is sinusoidal again, the harmonic currents are reduced. The activation of the virtual capacitor has only a small impact on the DC-link voltage.

VII. Conclusion

In this paper a novel concept for active damping for 3-phase rectifiers is proposed. An intelligent converter behavior is shown in which the input impedance has a frequency dependant nature. It is possible to actively damp filter resonances or move filter resonances out of problematic regions with a general virtual impedance concept. This can be used to maintain stability in a harsh environment with a distorted line. An extensive analysis with source and load impedance matrices was carried out to explain clearly the theoretical background. A time domain simulation showed the usability of this active damping with a capacitive resonance shift.

References

[1] A. Emadi, A. Khaligh, C. H. Rivetta, and G. A. Williamson, "Constant power loads and negative impedance instability in automotive systems: definition, modeling, stability, and control of power electronic converters and motor drives," *IEEE Trans. Veh. Technol.*, vol. 55, pp. 1112–1125, July 2006.

[2] R. D. Middlebrook, "Input filter considerations in design and application of switching regulators," in *Proc. IEEE Industry Applications Society Annual Meeting*, pp. 366–382, 1976.

[3] B. Bitenc and T. Seitz, "Optimizing dc power distribution network stability using root locus analysis," in *Proc. 25th International Telecommunications Energy Conference INTELEC '03*, pp. 691–698, 19–23 Oct. 2003.

[4] A. M. Rahimi and A. Emadi, "Active damping in dc/dc power electronic converters: A novel method to overcome the problems of constant power loads," *IEEE Trans. Ind. Electron.*, vol. 56, pp. 1428–1439, May 2009.

[5] M. Hoff, "Instability of power factor corrected power supplies with various ac sources," in *Proc. of the twenty-seventh international power conversion conference, PCIM93, Irvine California*, pp. 1–8, 1993.

[6] S. Hiti, D. Borojevic, R. Ambatipudi, R. Zhang, and Y. Jiang, "Average current control of three-phase pwm boost rectifier," in *Proc. 26th Annual IEEE Power Electronics Specialists Conference PESC '95 Record*, vol. 1, pp. 131–137, 18–22 June 1995.

[7] M. Chen and J. Sun, "Low-frequency input impedance models for boost single-phase pfc converters," in *Proc. IEEE 36th Power Electronics Specialists Conference PESC '05*, pp. 1062–1068, 16–16 June 2005.

[8] J. Sun and Z. Bing, "Input impedance modeling of single-phase pfc by the method of harmonic linearization," in *Proc. Twenty-Third Annual IEEE Applied Power Electronics Conference and Exposition APEC 2008*, pp. 1188–1194, 24–28 Feb. 2008.

[9] J. Sun, "Input impedance analysis of single-phase pfc converters," *IEEE Trans. Power Electron.*, vol. 20, pp. 308–314, Mar 2005.

[10] J. Sun, "Ac power electronic systems: Stability and power quality," in *Proc. 11th Workshop on Control and Modeling for Power Electronics COMPEL 2008*, pp. 1–10, 17–20 Aug. 2008.

[11] H. Mao, D. Boroyevich, and F. C. Lee, "Novel reduced-order small-signal model of three-phase pwm rectifiers and its application in control design and system analysis," in *Proc. 27th Annual IEEE Power Electronics Specialists Conference PESC '96 Record*, vol. 1, pp. 556–562, 23–27 June 1996.

[12] M. Belkhayat, *Stability Criteria For AC Power Systems With Regulated Loads*. PhD thesis, Purdue University, 1997.

[13] S. Gataric and N. R. Garrigan, "Modeling and design of three-phase systems using complex transfer functions," in *Proc. 30th Annual IEEE Power Electronics Specialists Conf. PESC 99*, vol. 2, pp. 691–697, 1999.

[14] L. Harnefors, "Modeling of three-phase dynamic systems using complex transfer functions and transfer matrices," *IEEE Trans. Ind. Electron.*, vol. 54, no. 4, pp. 2239–2248, 2007.

[15] S. Chandrasekaran, D. Borojevic, and D. K. Lindner, "Input filter interaction in three phase ac-dc converters," in *Proc. 30th Annual IEEE Power Electronics Specialists Conf. PESC 99*, vol. 2, pp. 987–992, 1999.

[16] J. Huang, K. Corzine, and M. Belkhayat, "Single-phase ac impedance modeling for stability of integrated power systems," in *Proc. IEEE Electric Ship Technologies Symposium ESTS '07*, pp. 483–489, 21–23 May 2007.

[17] Y. A. Familiant, J. Huang, K. A. Corzine, and M. Belkhayat, "New techniques for measuring impedance characteristics of three-phase ac power systems," *IEEE Trans. Power Electron.*, vol. 24, pp. 1802–1810, July 2009.

[18] J. Huang, K. A. Corzine, and M. Belkhayat, "Small-signal impedance measurement of power-electronics-based ac power systems using line-to-line current injection," *IEEE Trans. Power Electron.*, vol. 24, pp. 445–455, Feb. 2009.

[19] M. Liserre, F. Blaabjerg, and S. Hansen, "Design and control of an lcl-filter-based three-phase active rectifier," *IEEE Trans. Ind. Appl.*, vol. 41, pp. 1281–1291, Sept.–Oct. 2005.

[20] V. Blasko and V. Kaura, "A novel control to actively damp resonance in input lc filter of a three phase voltage source converter," in *Proc. 1996. Eleventh Annual Applied Power Electronics Conference and Exposition APEC '96*, vol. 2, pp. 545–551, 3–7 March 1996.

[21] P. A. Dahono, "A control method to damp oscillation in the input lc filter," in *Proc. IEEE 33rd Annual Power Electronics Specialists Conference pesc 02*, vol. 4, pp. 1630–1635, 23–27 June 2002.

[22] C. Wessels, J. Dannehl, and F. W. Fuchs, "Active damping of lcl-filter resonance based on virtual resistor for pwm rectifiers &stability analysis with different filter parameters," in *Proc. IEEE Power Electronics Specialists Conference PESC 2008*, pp. 3532–3538, 15–19 June 2008.

[23] A. S. Morsy, S. Ahmed, P. Enjeti, and A. Massoud, "An active damping technique for a current source inverter employing a virtual negative inductance," in *Proc. Twenty-Fifth Annual IEEE Applied Power Electronics Conf. and Exposition (APEC)*, pp. 63–67, 2010.

[24] S. D. Sudhoff, S. F. Glover, P. T. Lamm, D. H. Schmucker, and D. E. Delisle, "Admittance space stability analysis of power electronic systems," *IEEE Trans. Aerosp. Electron. Syst.*, vol. 36, no. 3, pp. 965–973, 2000.

[25] S. Hiti and D. Boroyevich, "Small-signal modeling of three-phase pwm modulators," in *Proc. 27th Annual IEEE Power Electronics Specialists Conf. PESC '96 Record*, vol. 1, pp. 550–555, 1996.